Involvement of variably-sourced fluids during the formation and later overprinting of Paleoproterozoic Au-Cu mineralization: Insights gained from a fluid inclusion assemblage approach

Erik L. Haroldson, Department of Geosciences, Austin Peay State University, Clarksville, TN, 37044 (haroldsone@apsu.edu)
Philip E. Brown, Department of Geoscience, University of Wisconsin-Madison, Madison, WI, 53706
Robert J. Bodnar, Fluids Research Lab, Department of Geosciences, Virginia Tech, Blacksburg, VA 24061

WISCONSIN
UNIVERSITY OF WISCONSIN–MADISON

Abstract

Au-Cu mineralized quartz veins of the Reef Deposit, Wisconsin, USA, originally formed prior to or early in the Paleoproterozoic Penokean orogeny in central North America as either the root zone of a gold-rich VMS deposit, or in an orogenic gold setting. Nearly 400 m.y. later, magmatic hydrothermal fluids associated with a continental scale anorogenic magmatic event remobilized mineralization within the veins. And still later, during the Paleozoic, remobilization and perhaps upgrading of Au and other metals occurred in response to circulation of fluids associated with Mississippi Valley-type deposits found in overlying supracrustal rocks. Fluid constraints on the formation of the Reef Deposit and later overprinting over a 1.5 b.y. timeframe are examined using the Fluid Inclusion Assemblage (FIA) approach. Distinctive assemblages are examined on individual merit, each offering individual stories to aid in our understanding of the protracted development of the Reef Deposit.

Presumably primary fluid inclusions in Au- and Cu-bearing quartz-sulfide veins that formed during the Paleoproterozoic event show H_2O-CO_2-CH_4±NaCl compositions based on microthermometry and laser Raman spectroscopy. Possibly primary H_2O-NaCl and secondary H_2O-CO_2-CH_4±NaCl FIA formed prior to regional deformation and are recognized as discrete relict and neonate clusters. The intersection of isochores from the highest density neonate inclusions of either fluid composition indicate re-equilibration at lower amphibolite conditions during regional deformation. Quartz hosted secondary fluid inclusion assemblages characterized by H_2O-CH_4 and CO_2-CH_4 compositions formed at high temperatures and have not been re-equilibrated and are interpreted to post-date regional metamorphism. These FIA occur along healed fractures with chalcopyrite mineralization. These inclusions are likely associated with fluid circulation driven by emplacement of the adjacent Wolf River Batholith (ca. 1.45 Ga), that altered pyrite to pyrrhotite and remobilized or emplaced chalcopyrite at temperatures as high as 700 °C. This reduced fluid was in equilibrium with locally observed graphitic sediments. Secondary lower temperature (< 50-210 °C) calcite and quartz hosted H_2O-NaCl inclusions show variable homogenization temperatures and salinities. H_2O-NaCl inclusions in quartz homogenize at 78-210 °C, with lower salinities of 3.0-13.9 wt. % NaCl equivalent, and are observed to crosscut CH4 bearing FIA. H_2O-NaCl inclusion assemblages in calcite have maximum homogenization temperatures of 103 °C and salinities of ~24 wt. % NaCl equiv. Lower temperature H_2O-NaCl inclusions are most likely related to the Paleozoic-aged MVT fluid overprint that remobilized and possibly emplaced gold mineralization.

Imagery:

Project Location

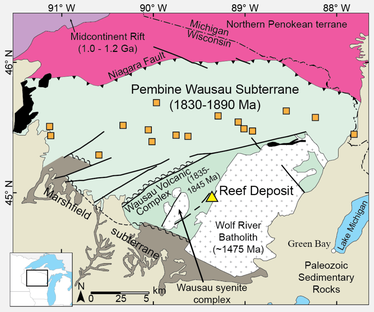

Figure 1. Simplified geologic map (modified from Cannon et al., 1997) of Pembine-Wausau subterrane and surrounding area. Triangle - the Reef Deposit, squares - volcanogenic massive sulfide deposits. Solid lines represent faults, squiggly lines represent shear zones. Black lithology areas represent Proterozoic quartzite, the dark grey Marshfield subterrane is Archean in age.

Cathodoluminescence

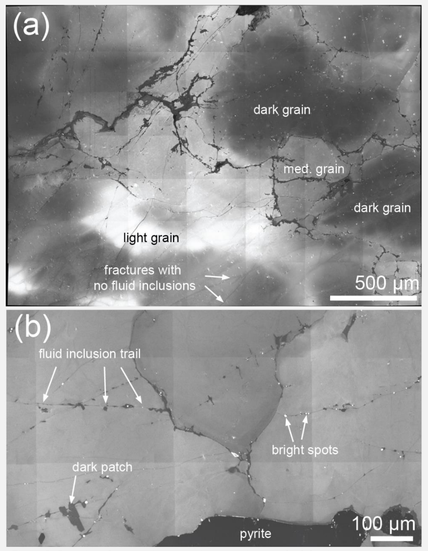

Figure 3. Scanning electron microscope images using a cathodoluminescence detector showing quartz textures discussed in the text. (a) image shows the presence of dark and light areas interpreted as relict quartz grains; gradational contact between dark and light areas was formed during recrystallization. (b) trace of secondary fluid inclusion bearing fractures as well as dark patches formed during morphological ripening (Lambrecht and Diamond, 2014). Bright spots indicate location of opened fluid inclusion leaving a depression that causes charging due to edge effects.

Veins

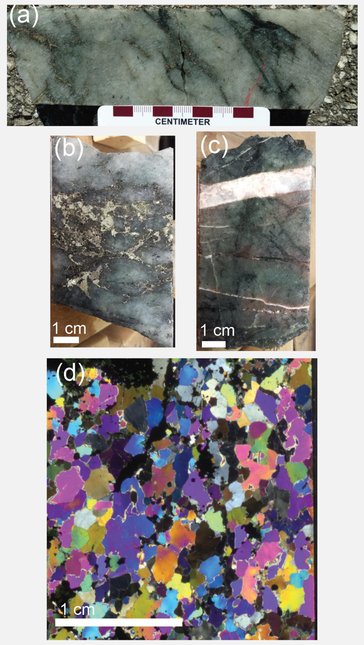

Figure 2. Photographs showing vein textures observed in the Reef Deposit. (a) typical quartz vein with sulfide and chlorite-filled fractures. (b) semi-massive sulfide consisting primarily of pyrrhotite with minor pyrite. (c) carbonate (calcite, dolomite) veinlet cross-cutting a primary quartz vein. (d) cross-polarized scanned image of fluid inclusion thick section showing commonly observed quartz texture.

Accidental Trapping, Relict/Neonate clusters, Secondary Trails

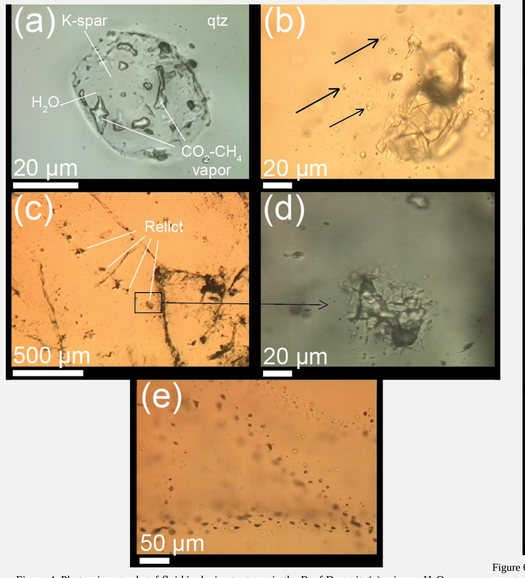

Figure 4. Photomicrographs of fluid inclusion textures in the Reef Deposit. (a) primary H_2O-CO_2-CH_4-NaCl fluid trapped accidentally at the interface between potassium feldspar and quartz. (b) relict H_2O- NaCl fluid inclusion surrounded by neonate inclusions (arrows) formed during deformation. (c) secondary trail of relict and neonate inclusion clusters. (d) relict H_2O-CO_2-CH_4-NaCl fluid inclusion from trail in image c. (e) secondary fluid inclusion trails. Photomicrographs a, and d are composite images of multiple focus levels.

Fluid Inclusions

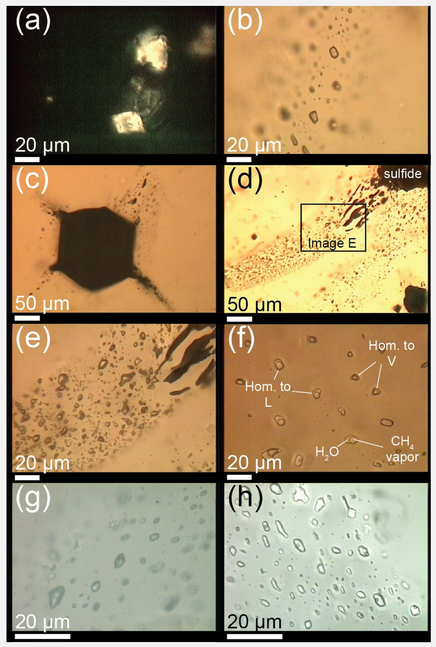

Figure 6. Photomicrographs of fluid inclusions in the Reef Deposit. (a) same area as in figure 4b in cross-polarized light showing birefringent solids. (b) vapor only inclusions identified as H_2O-CH_4. (c) vapor only fluid inclusions along secondary trails extending outward from pyrite and terminating in quartz. (d) vapor-only fluid inclusions along secondary trail extending outward from sulfide with irregularly shaped sulfides also formed along the secondary fracture. (e) zoomed image of area defined in image d showing details of vapor inclusions and sulfide. (f) fluid inclusion assemblage of H_2O-CH_4 inclusions some of which homogenize to vapor, others which homogenize to liquid. (g) fluid inclusion assemblage of CO_2-CH_4 inclusions. (h) fluid inclusion assemblage consisting of all liquid inclusions and two phase H_2O-NaCl inclusions hosted in quartz. Figures e, f and h are images created by blending multiple focal distances.

Distinctive assemblages are examined on individual merit, each offering individual stories to aid in our understanding of the protracted development of the Reef Deposit.

References

This content is published in Chemical Geology, please refer to the article for further citation information:
Haroldson, E.L., Brown, P.E., and Bodnar, R.J., Involvement of variably-sourced fluids during the formation and later overprinting of Paleoproterozoic Au-Cu mineralization: Insights gained from a fluid inclusion assemblage approach, Chemical Geology, 2018, vol. 497, p. 115-127, https://doi.org/10.1016/j.chemgeo.2018.08.027.

Acknowledgements

EH would like to thank Charles Farley of Virginia Tech for assistance in acquiring Raman microprobe data. Brian Hess prepared fluid inclusion thick sections. Philip Gopon assisted with SEM imaging. This research was supported by student research grants from the Society of Economic Geology – Canada Foundation and the Geological Society of America. Travel to Blacksburg was funded by UW-Madison Geoscience Department. EH thanks Aquila Resources Inc. for access to samples. Comments from Alexandre Tarantola, an anonymous reviewer and the editor helped to improve the manuscript.

~1830 Ma ~1470 Ma ~270 Ma

2000 1500 1000 500 Today

Methane bearing inclusions associated with ~1835 Ma vein formation (VMS or Orogenic Au?)

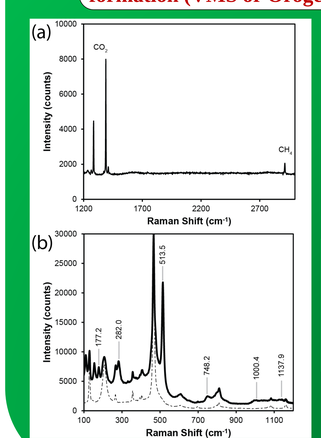

Figure 5. Raman spectra obtained from primary – type 1 fluid inclusion assemblages. (a) analysis of vapor bubble shows peaks for CO_2 and CH_4. (b) spectrum obtained from the solid phase associated with primary – type 1 fluid inclusions in this case is identified as potassium feldspar based on the Raman spectrum. Dashed line is spectrum of hosting quartz, solid line is potassium feldspar. Distinctive peaks not from host quartz closely match peaks for potassium feldspar in Lafuente et al. (2015).

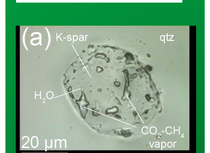

Amphibolite grade regional deformation identified by neonate inclusions

Figure 8. Isochores calculated from neonate inclusions of different compositions relict inclusions. Intersection of the highest density isochore (thick line) for H_2O-NaCl (light grey field) and H_2O-CO_2-CH_4-NaCl (dark grey field) composition relict inclusions approximate a typical orogenic geothermal gradient (30 °C/km) above 500 °C. H2O-NaCl isochore calculated from Bodnar and Vityk, (1994) in MacFlinCor (Brown and Hagemann, 1994). CO_2+CH_4 isochores for H_2O-CO_2-CH_4-NaCl calculated using equations from Bowers and Helgeson, (1985) in MacFlinCor (Brown and Hagemann, 1994). Orogenic geotherm is from figure 25.2 in Winter, (2010).

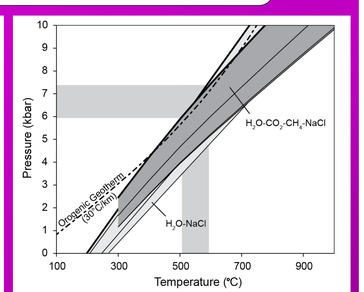

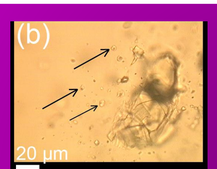

Methane bearing high temperature inclusions associated with ~1470 Ma magmatism

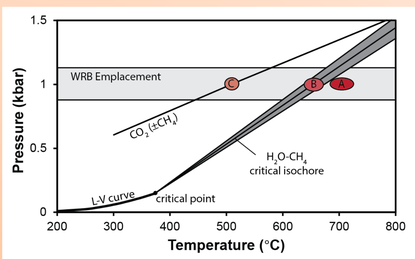

Figure 7. P-T diagram showing the fluid evolution during cooling of the Wolf River Batholith. At point A – A high temperature H_2O-CH_4 vapor is trapped. At point B - H_2O-CH_4 fluid is trapped in a range about the critical isochore (isochore values above and below the critical isochore are not calculated from equations of state and are schematic only). At point C - CO_2-CH_4 fluid is trapped at lower temperature. Estimate for Wolf River Batholith (WRB) emplacement is schematic using emplacement estimate of 3.8 km depth ≈ 1kbar (Anderson, 1980). H_2O-CH_4 critical isochore assumes negligible CH_4 concentration (table 2) and is calculated based on pure water using equations from Bodnar and Vityk, (1994) in MacFlinCor (Brown and Hagemann, 1994). The CO_2-CH_4 isochore is calculated using Swanenberg (1979).

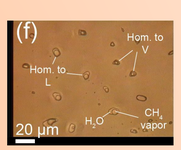

Low temperature H_2O-NaCl inclusions associated with late MVT overprint

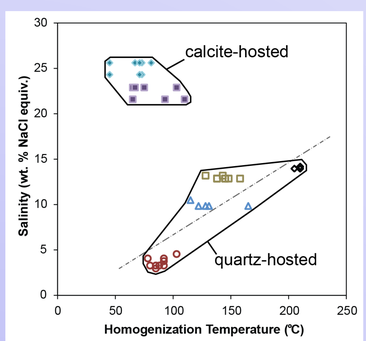

Figure 9. Homogenization temperature vs. salinity for type 6 fluid inclusion assemblages (FIA). Filled symbol – calcite-hosted fluid inclusion assemblage, open symbol – quartz-hosted FIA. Assorted shapes (or colors) represent individual fluid inclusion assemblages. Dashed trendline is for quartz-hosted FIA showing a correlation between increased salinity with increased homogenization temperature.

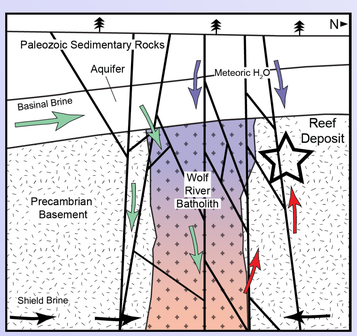

Figure 10. Schematic illustration of fluid flow paths from possible sources for late Paleozoic fluid (type 6 fluid) flow responsible for mineralization/remobilization of gold in the Reef Deposit (not to scale). Basinal brine fluids are derived from typical Mississippi Valley-type gravity driven fluid flow model. Shield Brine fluids form from stagnant fluid in deep crustal basement terranes. Meteoric water represents a lower temperature and lower salinity fluid. Color gradient in Wolf River Batholith illustrates a temperature gradient, with high temperatures forming at depth by radioactive decay (Spirakis and Heyl, 1996).